IEEE Access
Multidisciplinary | Rapid Review | Open Access Journal

Received August 14, 2017, accepted September 9, 2017, date of publication September 14, 2017,
date of current version October 12, 2017.

Digital Object Identifier 10.1109/ACCESS.2017.2752210

Analysis of a Wideband Circularly Polarized Cylindrical Dielectric Resonator Antenna With Broadside Radiation Coupled With Simple Microstrip Feeding

RAKESH CHOWDHURY, (Student Member, IEEE), NAVEEN MISHRA, (Student Member, IEEE), MOHAMMED MUZAMMIL SANI, (Student Member, IEEE), AND RAGHVENDRA KUMAR CHAUDHARY, (Member, IEEE)
Indian Institute of Technology (Indian School of Mines), Dhanbad 826004, India
Corresponding author: Rakesh Chowdhury (rc4076@gmail.com)

ABSTRACT In this paper, a wideband circularly polarized cylindrical shaped dielectric resonator antenna (DRA) with simple microstrip feed network has been designed and investigated. The proposed design uses dual vertical microstrip lines arranged in a perpendicular fashion to excite fundamental orthogonal hybrid $HE^{x}_{11\delta}$ and $HE^{y}_{11\delta}$ modes in the cylindrical DR. The Phase quadrature relationships between orthogonal modes have been attained by varying corresponding microstrips heights. To ratify the simulation results, an antenna prototype is fabricated and measured. Measured input reflection coefficient and axial ratio bandwidth (at $\Phi = 0°, \theta = 0°$) of 30.37% (2.82–3.83 GHz) and 24.6% (2.75–3.52 GHz) has been achieved, respectively. This antenna design achieves an average gain of 5.5 dBi and radiation efficiency of above 96% over operational frequency band. Justifiable agreement between simulated and fabricated antenna results are obtained.

INDEX TERMS Circular polarization, dielectric resonator, wideband antenna.

I. INTRODUCTION

The application of dielectric resonators (DRs) as an efficient radiator was introduced by Long *et al.* in 1983 [1]–[3]. Since then DRs have been fully scrutinized for antenna applications at microwave frequencies. It offers various inherent attractive features over microstrip antennas which includes higher radiation efficiency, absence of surface waves, easy integration with existing technology etc. [4], [5]. Initially, research was focused on designing of linearly polarized (LP) antennas. But with rapid growth of wireless communications, better signal connection becomes an indispensable task. The use Circularly polarized (CP) antennas ensures the successful link between transmitter and receiver. This is because, CP antennas provides better quality of signals, immunity from faraday rotation in ionosphere making it suitable for space applications, flexibility in transmitter and receiver antenna orientation etc. [6].

The research on circularly polarized dielectric resonator antennas (CP-DRA) was started in 1990s. At the beginning, complex feed networks were employed to obtain wide axial ratio bandwidth such as Wilkinson power dividers, and dual port networks [7]–[9]. These methods have complex set-ups and impractical for use. In order to remove the complexity, researchers have explored new techniques to generate CP with simple feed network. In this connections, various techniques were proposed using single feed excitation to realize wideband CP antenna. In [10], a single feed wideband CP was reported where 24% of axial ratio bandwidth (ARBW) has been achieved using perturbation technique. But realization of this method is difficult due to fabrication limitations. A trapezoidal shaped DRA was reported in [11] which offers 21.5% ARBW. But these types of dielectric resonators are very hard in nature and difficult to malleable in any shape using simple machining. In literature [12], a probe fed slotted wideband CP-DRA was presented, which shows 25% of ARBW. A simple shaped DRA with 20.62% of ARBW and low gain has been presented in [13].

In this article, a wideband circularly polarized cylindrical dielectric resonator antenna (CDRA) based on a single feed

excitation is investigated. In this work, a simple cylindrical shaped dielectric resonator is used which is easily available. Proposed antenna configuration and design details are given in Section II. The procedure adopted for designing this CP antenna are properly explained in Section III with the help of field distributions. To get optimum wideband performance, parametric studies have been performed as shown in Section IV. In Section V, measurement results are discussed to verify the practical antenna performance. Finally, this antenna is compared with some recently published single fed wideband circularly polarized antennas followed by conclusions given in Section VI.

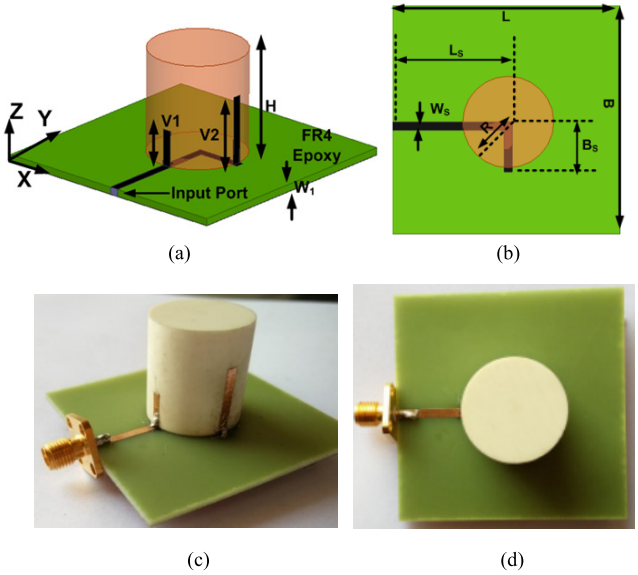

FIGURE 1. Schematic and prototype of proposed circularly polarized cylindrical dielectric resonator antenna. (a) 3D-view of proposed structure. (b) Top-view of proposed structure. (c) 3D-view of antenna prototype. (d) Top view of antenna prototype. (All dimension are in mm: $R = 11$, $H = 23$, $V1 = 9$, $V2 = 15$, $W_1 = 1.6$, $L = B = 55$, $L_S = 28$, $B_S = 13$, $W_S = 1.8$.)

II. ANTENNA SET-UP AND DESIGN EQUATIONS

The schematic diagram of proposed antenna composition is shown in Fig.1(a) and Fig. 1(b). An antenna prototype has been fabricated for validation purpose and shown in Fig. 1(c) and Fig. 1(d) respectively. The antenna geometrical values are provided in the caption of Fig.1. The radiator part of proposed composition consists of a cylindrical shaped ceramic material having permittivity of 9.8. It has dimensions of height 'H' and radius 'R'. The whole antenna structure is settled over a FR4 epoxy substrate ($\varepsilon_r = 4.4$, $\tan\delta = 0.025$) on top of an L x B mm^2 full ground plane. To excite the dielectric resonator, dual vertical microstrip lines (called as V1 and V2) have been attached to the DR in space quadrature to generate orthogonal modes in the structure. Thereafter, to obtain 90° phase difference between orthogonal modes, microstrips heights are varied. This feeding mechanism does not require complex circuitry, still provides wide axial ratio, consistent gain and good radiation efficiency over operational frequency band. To calculate the dimensions of dielectric resonator for a given resonant frequency (f_{res}) of fundamental mode, subsequent empirical formulas have been used in literature [5].

$$f_{res} = \frac{6.321c}{\pi d\sqrt{\varepsilon_{eff}+2}}\left[0.27+0.36\left(\frac{d}{4h_{eff}}\right)+0.02\left(\frac{d}{4h_{eff}}\right)^2\right] \quad (1)$$

Where ε_{eff} is the effective permittivity of the whole antenna structure, d is the diameter of cylindrical DR, h_{eff} is the total height of proposed structure, Where ε_{eff} and h_{eff} has been found by using following formulas

$$\varepsilon_{eff} = \frac{h_{eff}}{\frac{h_{dra}}{\varepsilon_{CDRA}} + \frac{h_{Sub}}{\varepsilon_{sub}}} \quad (2)$$

$$h_{eff} = h_{dra} + h_{Sub} \quad (3)$$

Where h_{dra} and h_{Sub} corresponds to height of DR and substrate whereas ε_{CDRA} and ε_{CDRA} corresponds to dielectric constant of DR and substrate respectively.

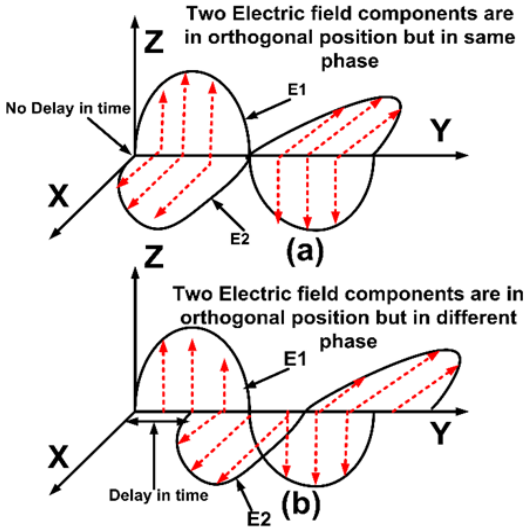

FIGURE 2. Generation of circularly polarized wave. (a) Two electric field components separated in space (orthogonal signals). (b) Two orthogonal electric field components with time delay (to establish phase difference between them).

III. THEORETICAL BACKGROUND AND DESIGN APPROACH

A circularly polarized (CP) wave can be generated inside DRA by exciting two orthogonal components of electric field in phase quadrature. Fig. 2 shows the mechanism to generate a CP wave. Generation of orthogonal E-field components is primary requirement that requires two linearly polarized electric field components (let us say E1 and E2) separated by 90° in space as shown in Fig. 2(a). Next, essential requirement is establishing phase quadrature relationship between both components which in turn requires separation of orthogonal components in time. Fig. 2(b) shows the time delay between E1 and E2 that causes phase difference

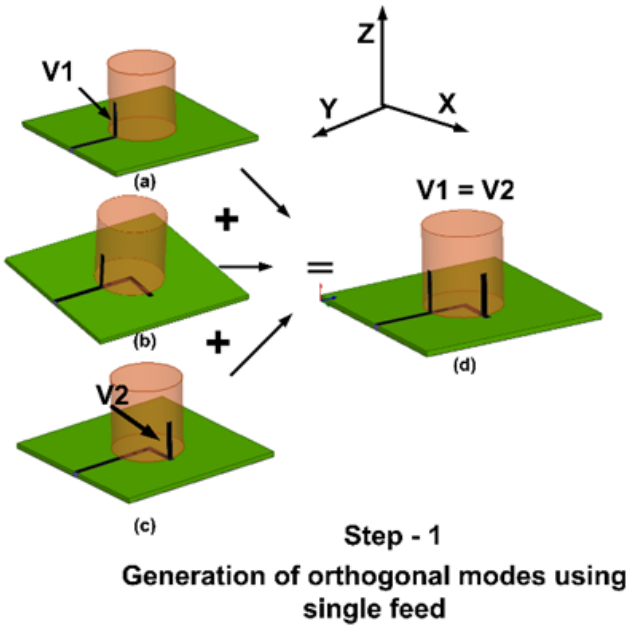

FIGURE 3. Proposed methodology adopted to design proposed CP antenna. (a) CDRA with microstrip V1 only. (b) CDRA with microstrip V1 and L-shaped strip only. (c) CDRA with microstrip V2 and L-shaped horizontal strip only. (d) CDRA with both microstrip V1 and V2 of same height.

between them. By employing such conditions the resultant electric field rotates in a circular manner at a particular point as time varies, resulting in circular polarization.

In this work, orthogonal E-field components are generated with the help of dual vertical microstrip lines called as V1 and V2 in this paper. Phase quadrature relationship between them is obtained by varying their corresponding heights. The entire procedure for CP generation is elaborated in following two steps: (a) Step-1: Generation of orthogonal modes in DR (b) Step-2: Obtaining phase quadrature relationship between orthogonal modes.

A. STEP-1 (GENERATION OF ORTHOGONAL MODES IN CDRA)

The entire procedure adopted to generate orthogonal modes in cylindrical DR is depicted in Fig. 3(a) to Fig. 3(d). Initially, fundamental mode $\boldsymbol{HE^{x}_{11\delta}}$ is excited by placing a vertical microstrip line V1 (with height of 12 mm) at the edge of cylindrical DR as shown in Fig. 3(a). Fig. 4(a) shows the input reflection coefficient when V1 is connected. It can be seen that resonance is obtained at 2.97 GHz which corresponds to $\boldsymbol{HE^{x}_{11\delta}}$ mode. The electric field distribution is plotted inside DRA due to strip V1 only at 2.97 GHz and shown in Fig. 5(a). This mode behaves like an x-directed horizontally placed magnetic dipole. In next step, an L-shaped horizontal microstrip line is added to V1 beneath the CDRA as shown in Fig. 3(b). After adding this horizontal microstrip line, input reflection coefficient plot is not affected but matching deteriorates as shown in Fig. 4(b). This shows that addition of L-shaped microstrip line has not affected the resonance position of $\boldsymbol{HE^{x}_{11\delta}}$ mode but

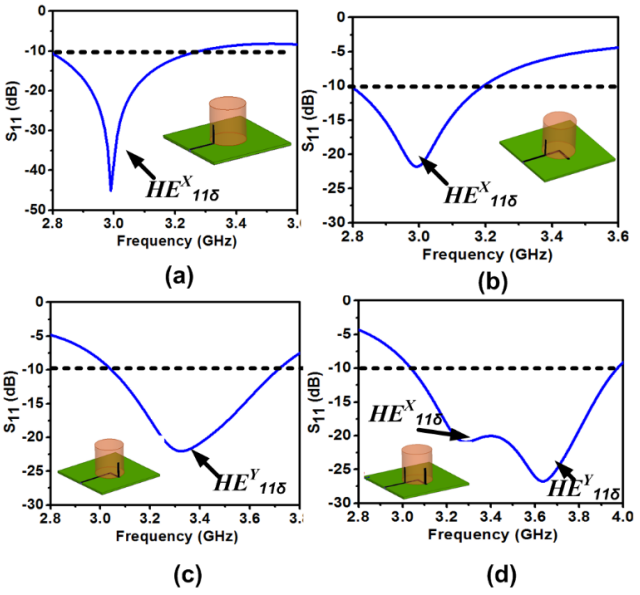

FIGURE 4. Simulated input reflection coefficient. (a) CDRA with microstrip V1 only. (b) CDRA with microstrip V1 and L-shaped strip only. (c) CDRA with microstrip V2 and L-shaped horizontal strip only. (d) CDRA with both microstrip V1 and V2 of same height.

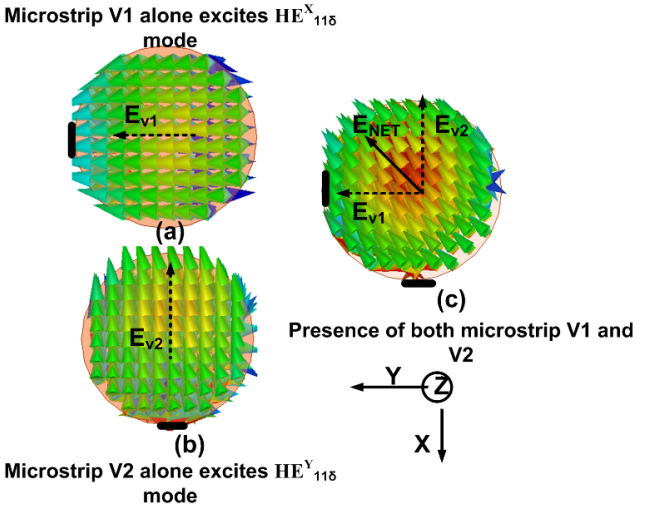

FIGURE 5. Simulated electric field distribution considering at 3.2 GHz. (a) Microstrip V1 only. (b) Microstrip V2 only. (c) Both microstrips V1 and V2.

only coupling is altered. In Fig. 3(c), a second vertical microstrip line V2 is added in space quadrature with same height as of V1 while removing V1. Fig 4(c) shows the input reflection coefficient plot considering V2 strip only where resonance is obtained at 3.3 GHz. Considering this arrangement the electric field pattern developed is displayed in Fig. 5(b) due to V2 only and mode $\boldsymbol{HE^{y}_{11\delta}}$ is observed. This microstrip V2 would generate $\boldsymbol{HE^{y}_{11\delta}}$ mode (orthogonal to $\mathbf{HE^{x}_{11\delta}}$ mode) as shown in Fig. 5(b). This mode behaves like a y-directed horizontally placed magnetic dipole. To excite simultaneously these orthogonal modes both microstrip lines V1 and V2 are connected simultaneously by using the L-shaped microstrip (beneath of DR) as shown in Fig. 3(d). In Fig. 4(d) two frequency points (where S_{11} is below -20 dB)

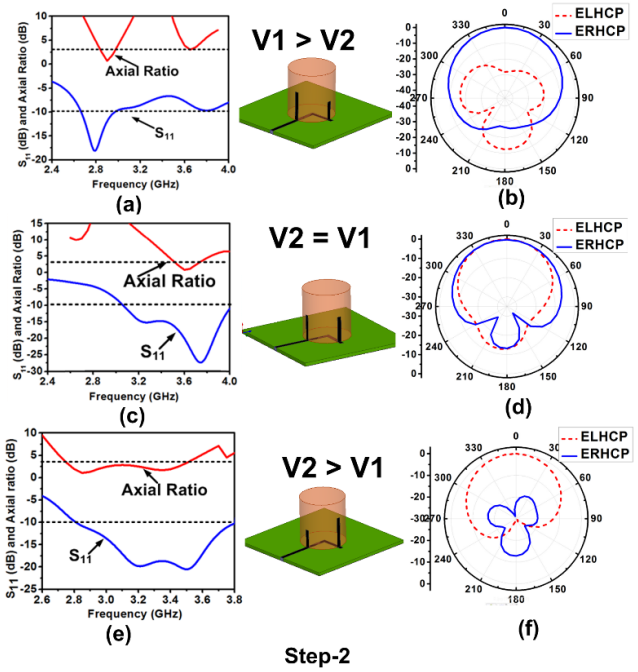

FIGURE 6. Procedure to achieve phase quadrature relationship. (a) Simulated input reflection coefficient and axial ratio for V1 > V2. (b) Simulated radiation pattern at 2.9 GHz for V1 > V2 showing RHCP mode. (c) Simulated input reflection coefficient and axial ratio for V2 = V1 (d) Simulated radiation pattern at 2.9 GHz for V2 = V1 showing Linearly polarized behaviour. (e) Simulated input reflection coefficient and axial ratio for V2 > V1. (f) Simulated radiation pattern at 2.9 GHz for V2 > V1.

have been observed which corresponds to these two modes i.e. $\mathbf{HE}^{\mathbf{x}}_{11\delta}$ and $\boldsymbol{HE}^{\boldsymbol{y}}_{11\delta}$. Hence two field pattern are generated inside CDRA with the help of two vertical microstrip lines which are separated in space by 90°.

Fig. 5(c) shows the electric field distribution inside cylindrical DR considering microstrip line V1 and V2 simultaneously. With reference to Fig. 5(c), it has been observed that, when both microstrips V1 and V2 are considered together, the direction of net electric field (E_{NET}) is oriented at 45°. This shows that net electric field is composed of two orthogonal components where one component is generated due to V1 in y-direction and other due to V2 in x-direction.

B. STEP-2 (ACHIEVING PHASE DIFFERENCE BETWEEN ORTHOGONAL MODES)

After generation of orthogonal modes in CDRA, it is required to create some time delay between them in order to build phase quadrature relationship to generate CP. This is done by varying the height of vertical microstrip lines V1 and V2 as shown in Fig. 6. There are three cases possible: (i) V1 > V2, (ii) V1 = V2 and (iii) V2 > V1. Fig. 6(a), Fig. 6(c) and Fig. 6(e) shows the input impedance bandwidth for V1 > V2, V1 = V2 and V2 > V1 respectively. It has been observed that for V1 > V2, both modes are not properly excited and a narrowband CP of 6% (2.84-3 GHz) is generated. In the case when V2 > V1 and V1 = V2, both modes are properly excited

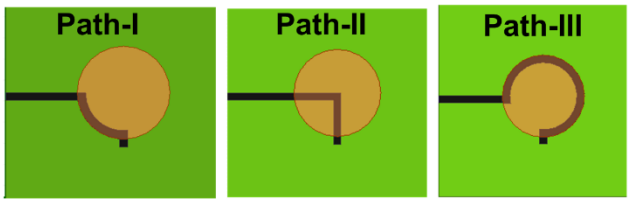

FIGURE 7. Different shaped horizontal strip for connecting vertical strip V1 and vertical strip V2. (a) Path-I. (b) Path-II (chosen for designing final proposed antenna). (c) Path-III.

and wideband CP is achieved in those configurations. So later configuration (V2 > V1) is chosen to design proposed wideband CP antenna. The optimal values of microstrip heights are found by parametric studies. In this composition, by varying the relative height, path difference between two strips can be varied. So, $\pm\pi/2$ phase difference is obtained by adjusting their heights according to the equation (4). The effect of this height variation is observed in radiation pattern plotted at 2.9 GHz. It has been observed from Fig. 6(b) and 6(f) that RHCP mode is generated when V1 > V2 while LHCP mode is generated when V2 > V1. When both strip are considered as V1 = V2, then LHCP and RHCP modes are superimposed giving rise to linear polarized behavior

$$Phase\ difference = \frac{2\Pi}{\lambda} * Path\ difference \tag{4}$$

IV. PARAMETRIC STUDIES

In this section, parametric analysis has been carried out by using Ansys HFSS software version 14.0 to find the optimal values to design wideband CP antenna with best performance. By altering the parameters of this antenna composition, axial ratio and input reflection coefficient can be easily tuned for desired output. During parametric studies one parameter is kept varying while keeping all others parameters fixed.

A. EFFECT OF DIFFERENT SHAPED HORIZONTAL STRIP CONNECTING V1 AND V2

In the proposed configuration, vertical strip V1 and strip V2 is responsible for generation of orthogonal modes. These strips are connected by a horizontal L-shaped microstrip feed. There are some different ways also possible to connect V1 and V2 which are named as path I, path II and path III as shown in Fig. 7. Fig.8 shows the input reflection coefficient behavior for different paths to connect V1 and V2. It has been observed that path-I and path-III are not properly coupled with the dielectric resonator whereas with path-II, maximum coupling and good matching is achieved. The reason for this is explained as follows: In proposed CDRA, fundamental modes $\boldsymbol{HE}^{\boldsymbol{x}}_{11\delta}$ and $\boldsymbol{HE}^{\boldsymbol{y}}_{11\delta}$ are excited whose field strengths are maximum at the middle and gradually decreases along the circumference of CDRA. So, to connect V1 and V2, path-II is chosen to design proposed antenna.

B. EFFECT OF PERMITTIVITY (ε_r) OF CDRA

Fig. 9(a) and Fig. 9(b) shows the simulated input reflection coefficient and axial ratio when the permittivity of dielectric

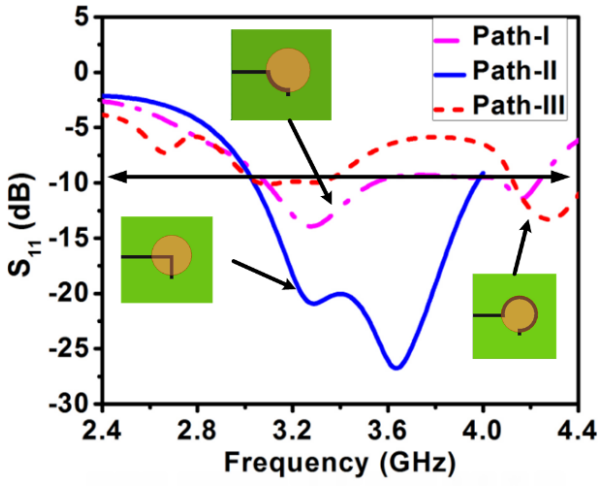

FIGURE 8. Simulated input reflection coefficient for different shaped horizontal paths.

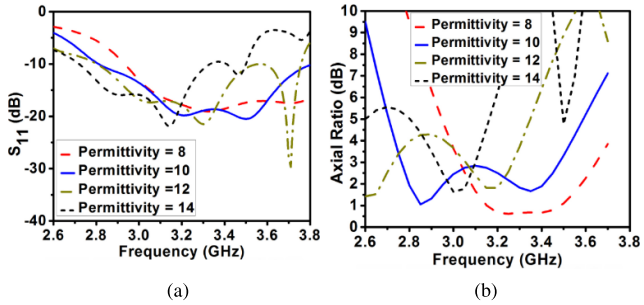

FIGURE 9. Simulation results of parametric analysis. (a) Input reflection coefficient with varying permittivity. (b) Axial ratio with varying permittivity.

resonator is varied. With reference to Fig. 9, the impedance bandwidth decreases with increase of permittivity. This is because, with increase in permittivity energy confinement within DR is more so quality factor increases which in turn reduces the impedance bandwidth. The axial ratio bandwidth also shows very large variations for different values of permittivity. At $\varepsilon_r = 10$, best CP performance is obtained. Due to unavailability of DR material with $\varepsilon_r = 10$, a value of 9.8 is used to design the CP antenna for getting wideband performance.

C. EFFECT OF MICROSTRIP WIDTH (W_S)

The effect of microstrip width (Ws) on input reflection coefficient and axial ratio is shown in Fig. 10(a) and 10(b) respectively. It has been noticed that at width of 2 mm and 2.2 mm, the axial ratio is close to 3 dB, so this value is not chosen to design practical antenna. By taking width of 1.6 mm and 1.8 mm, both providing axial ratio near about 3 dB but between them poor matching is provided by width of 1.6 mm. So from the study of both plots width of 1.8 mm is chosen to design practical CP antenna.

D. EFFECT OF MICROSTRIP HEIGHT V1 AND V2

The influence of microstrip height V1 and V2 on input reflection coefficient and axial ratio is depicted in Fig. 11 and

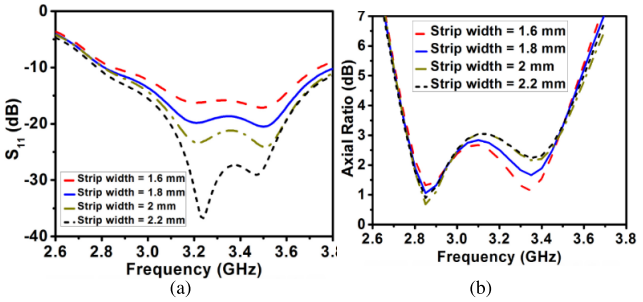

FIGURE 10. Simulation results of parametric analysis. (a) Input reflection coefficient with varying strip width. (b) Axial ratio with varying strip width.

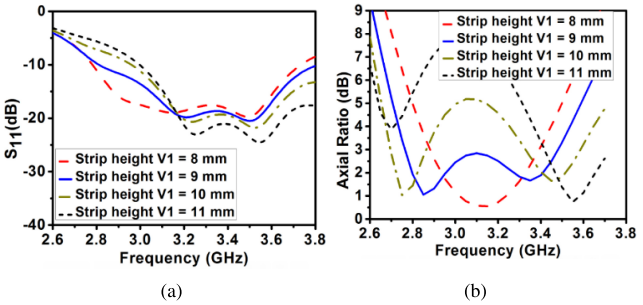

FIGURE 11. Simulation results of parametric analysis. (a) Input reflection coefficient with varying strip height V1 .(b) Axial ratio with varying strip height V1.

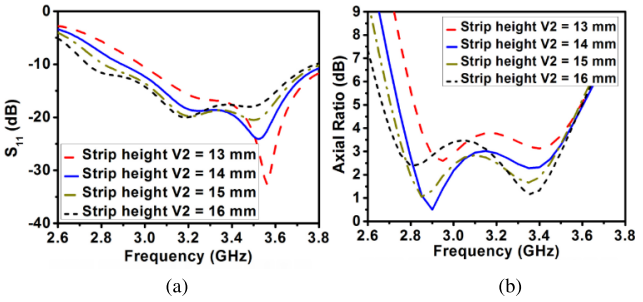

FIGURE 12. Simulation results of parametric analysis. (a) Input reflection coefficient with varying strip height V2. (b) Axial ratio with varying strip height V2.

Fig. 12. Fig. 11(b) clearly illustrates that axial ratio bandwidth is strongly dependent on microstrip height V1. This is because, the phase quadrature relationship is achieved by varying the heights of vertical microstrip lines as discussed in previous section. So for microstrip V1, value of 9 mm is chosen. Fig. 12(b) shows the effect of varying V2 which also affects axial ratio. Both microstrip heights can be easily tuned for better matching as can be seen from Fig. 11(a) and Fig. 12(a). To design CP antenna for wideband performance the final microstrip heights are chosen as V1 = 9 mm and V2 = 15 mm respectively.

V. MEASURED RESULTS AND DISCUSSION

In order to verify the simulation results, an antenna model has been fabricated and tested.

A. INPUT REFLECTION COEFFICIENT

The measurements for input reflection coefficient was done by using an Agilent E5071C vector network analyzer. The simulated and measured -10 dB input impedance bandwidth

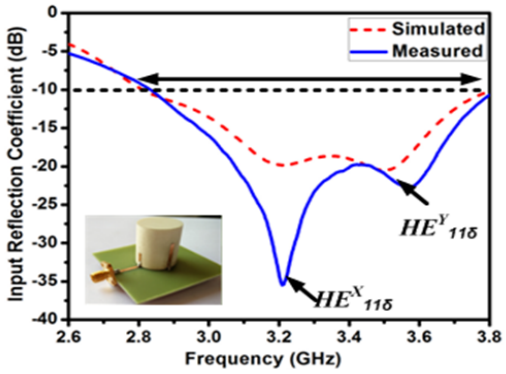

FIGURE 13. Simulated and measured input reflection coefficient of final proposed antenna.

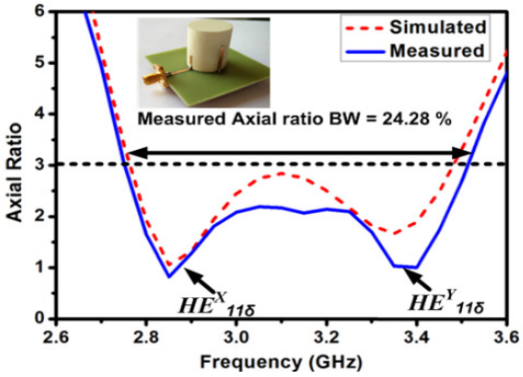

FIGURE 14. Simulated and measured axial ratio ($(\Phi = 0°, \theta = 0°)$ of final proposed antenna.

of 29.78% (2.8 – 3.78 GHz) and 30.37% (2.82 – 3.83 GHz) has been obtained respectively in this design as shown in Fig. 13. The two peaks corresponds to $\boldsymbol{HE^{x}_{11\delta}}$ and $\boldsymbol{HE^{y}_{11\delta}}$ mode. A little amount of discrepancy in matching can be noticed in the plot which may be due to the non-uniformity of substrate, quality of connectors, fabrication error subjected to soldering inaccuracy of vertical copper microstrips with horizontal copper strips.

B. AXIAL RATIO

Fig. 14 shows the simulated and measured axial ratio bandwidth of 23.07% (2.76 – 3.48 GHz) and 24.6% (2.75 – 3.52 GHz) respectively in broadside direction ($\Phi = 0°$, $\theta = 0°$). The two lower peaks in axial ratio plot corresponds to orthogonal modes $\boldsymbol{HE^{x}_{11\delta}}$ and $\boldsymbol{HE^{y}_{11\delta}}$. Due to merging of these modes wideband CP is achieved in the structure.

C. RADIATION PATTERN

The far field measurements have been performed in an anechoic chamber. The radiation patterns for proposed antenna are shown in Fig. 15 at two different frequencies in xz plane. Radiation pattern is plotted at 2.85 GHz and 3.35 GHz for which proposed antenna shows minimum axial ratio value. It has been observed that left handed circularly polarized waves (LHCP) are more dominant then right handed circularly polarized waves (RHCP) in broadside direction. Hence, this proposed antenna design is an LHCP antenna. LHCP and

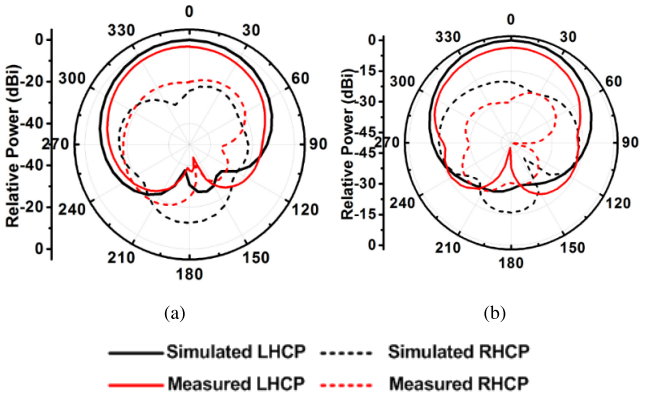

FIGURE 15. Simulated and measured radiation pattern of final proposed antenna. (a) XZ-Plane at 2.85 GHz. (b) XZ-Plane at 3.35 GHz.

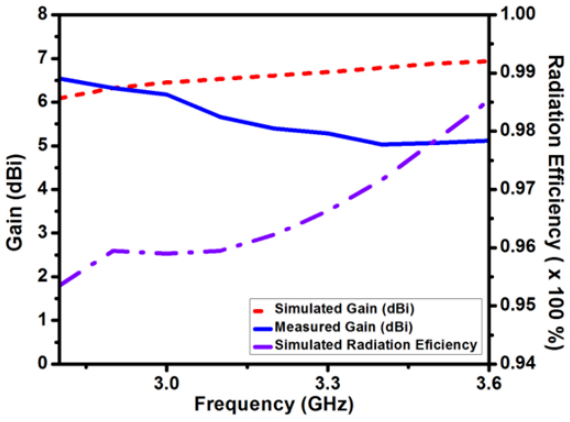

FIGURE 16. Simulated and measured gain with simulated radiation efficiency of final proposed antenna.

RHCP patterns are plotted using equation 5 and 6 [6]. It has been found that LHCP fields are stronger then RHCP fields in broadside direction approximately by 18 dB (2.85 GHz) and 17 dB (3.35 GHz) respectively in xz-plane.

$$E_{RHCP} = 0.707(E_{Hor} + jE_{Ver}) \quad (5)$$

$$E_{LHCP} = 0.707(E_{Hor} - jE_{Ver}) \quad (6)$$

D. GAIN AND RADIATION EFFICIENCY

The measured and simulated gains with simulated radiation efficiency of this antenna composition are plotted in Fig. 16. This design has achieved an average gain of 5.5 dBi in broadside direction. It also provides very good efficiency above 96% in the working range.

E. ELECTRIC FIELD DISTRIBUTION

In Fig. 17, the electric field distribution is demonstrated inside CDRA for different phase angles (0°, 60°, 120°, 180°, 240° and 300°) at 3.2 GHz, which shows clockwise motion of electric field. So it also confirms the generation of LHCP waves.

F. COMPARISON WITH RECENTLY PUBLISHED WORK

The proposed antenna is compared with recently published single feed wideband circularly polarized DRAs and

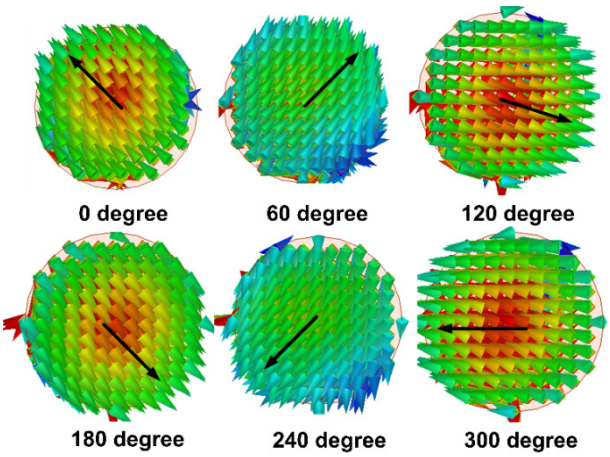

FIGURE 17. Simulated electric field distribution inside final proposed configuration at different phase angles at 3.2 GHz.

TABLE 1. Comparison of proposed design with recently published papers.

Ref.	Shape (ε_r)	Usable AR BW%	Height (mm)	Feed	Gain (dBi)
[14]	Rectangle (9.8)	14.46	$0.26\lambda_0$	Microstrip	6.4
[15]	Rectangle (9.8)	18.2	$0.16\lambda_0$	Aperture	4.5
[13]	Rectangle (9.8)	20.62	$0.23\lambda_0$	Microstrip	1.5
[11]	Trapezoidal(9.4)	21	$0.41\lambda_0$	Aperture	>5.2
[16]	Rectangle (10.2)	22	$0.23\lambda_0$	Microstrip	5.2
[12]	Slotted Rectangle (15)	22	$0.48\lambda_0$	Probe	1.48
This Work	Cylinder (9.8)	24.6	$0.22\lambda_0$	Microstrip	5.5

illustrated in Table 1. From Table 1, it has been concluded that proposed CP design is better in terms of both higher axial ratio bandwidth and consistent gain throughout the working frequency band.

VI. CONCLUSION

In this paper, a single feed circularly polarized cylindrical dielectric resonator antenna has been designed and demonstrated for wideband circular polarization applications. For realizing circular polarization in the structure, a pair of vertical microstrip lines have been used in perpendicular arrangement to excite orthogonal modes whereas phase quadrature relationship has been obtained by varying their respective heights. Fundamental hybrid $\boldsymbol{HE^{x}_{11\delta}}$ and $\boldsymbol{HE^{y}_{11\delta}}$ modes are responsible for generating conditions for circular polarization in the structure. A practical antenna model is fabricated to verify simulation results where good agreement between them has been observed. The proposed design provides 30.37% (2.82–3.83 GHz) of measured input impedance bandwidth. It also offers 24.6% (2.75–3.52 GHz) of measured axial ratio bandwidth. The far field results are found to be consistent in the working frequency range. This design can be used for airport surveillance radar (2.7-2.9 GHz) and Wi-MAX applications (3.3-3.6GHz)

REFERENCES

[1] S. A. Long, M. McAllister, and L. Shen, "The resonant cylindrical dielectric cavity antenna," *IEEE Trans. Antennas Propag.*, vol. AP-31, no. 3, pp. 406–412, May 1983.
[2] M. W. McAllister, S. A. Long, and G. L. Conway, "Rectangular dielectric resonator antenna," *Electron. Lett.*, vol. 19, no. 6, pp. 218–219, Mar. 1983.
[3] M. W. McAllister and S. A. Long, "Resonant hemispherical dielectric antenna," *Electron. Lett.*, vol. 20, no. 16, pp. 657–659, Aug. 1984.
[4] A. Petosa, *Dielectric Resonator Antenna Handbook*. Norwood, MA, USA: Artech House, 2007.
[5] R. K. Mongia and P. Bhartia, "Dielectric resonator antennas—A review and general design relations for resonant frequency and bandwidth," *Int. J. RF Microw Millim. Comput.-Aided Eng.*, vol. 4, no. 3, pp. 230–247, 1994.
[6] B. Y. Toh, R. Cahill, and V. F. Fusco, "Understanding and measuring circular polarization," *IEEE Trans. Edu.*, vol. 46, no. 3, pp. 313–318, Aug. 2003.
[7] S. L. S. Yang, R. Chair, A. A. Kishk, K. F. Lee, and K. M. Luk, "Study on sequential feeding networks for subarrays of circularly polarized elliptical dielectric resonator antenna," *IEEE Trans. Antennas Propag.*, vol. 55, no. 2, pp. 321–333, Feb. 2007.
[8] B. Li, C. X. Hao, and X. Q. Sheng, "A dual-mode quadrature-fed wideband circularly polarized dielectric resonator antenna," *IEEE Antennas Wireless Propag. Lett.*, vol. 8, pp. 1036–1038, 2009.
[9] S. Fakhte, H. Oraizi, and R. Karimian, "A novel low-cost circularly polarized rotated stacked dielectric resonator antenna," *IEEE Antennas Wireless Propag. Lett.*, vol. 13, pp. 722–725, 2014.
[10] P. Patel, B. Mukherjee, and J. Mukherjee, "Wideband circularly polarized rectangular dielectric resonator antennas using square-shaped slots," *IEEE Antennas Wireless Propag. Lett.*, vol. 15, pp. 1309–1312, 2016.
[11] Y. Pan and K. W. Leung, "Wideband circularly polarized trapezoidal dielectric resonator antenna," *IEEE Antennas Wireless Propag. Lett.*, vol. 9, pp. 588–591, 2010.
[12] Y. M. Pan and K. W. Leung, "Wideband omnidirectional circularly polarized dielectric resonator antenna with parasitic strips," *IEEE Trans. Antennas Propag.*, vol. 60, no. 6, pp. 2992–2997, Jun. 2012.
[13] R. Kumar and R. K. Chaudhary, "A wideband circularly polarized cubic dielectric resonator antenna excited with modified microstrip feed," *IEEE Antennas Wireless Propag. Lett.*, vol. 15, pp. 1285–1288, 2016.
[14] R. Chowdhury and R. K. Chaudhary, "Wideband circularly polarized rectangular DRA fed with dual pair of right-angled microstrip line," *Int. J. RF Microw. Millim. Comput.-Aided Eng.*, vol. 26, no. 8, pp. 713–723, 2016.
[15] K. X. Wang and H. A. Wong, "Circularly polarized antenna by using rotated-stair dielectric resonator," *IEEE Antennas Wireless Propag. Lett.*, vol. 14, pp. 787–790, 2015.
[16] S. Fakhte, H. Oraizi, R. Karimian, and R. Fakhte, "A new wideband circularly polarized stair-shaped dielectric resonator antenna," *IEEE Trans. Antennas Propag.*, vol. 63, no. 4, pp. 1828–1832, Apr. 2015.

RAKESH CHOWDHURY (S'16) was born in West Bengal, India, in 1991. He received B. Tech. degree in electronics and communication engineering from WBUT University, West Bengal, in 2013, the M. Tech. degree from the Indian Institute of Technology (Indian School of Mines), Dhanbad, in 2015, where he got fellowship from the Ministry of Human Resource Development Government of India. He is currently pursuing the Ph.D. degree with the Indian Institute of Technology (Indian School of Mines), Dhanbad. He has authored or co-authored over ten research articles in international journals/ conference proceedings. His current research interest includes circularly polarized dielectric resonator antennas, High gain antennas, and EBG structures. He also received certificate of Honour for excelling in academics during graduation. He is a potential reviewer of many journals, such as the IEEE Antenna and Wireless Propagation Letters, the IEEE Access, *International Journal of RF and Microwave Computer Aided Engineering*.

NAVEEN MISHRA was born in Deoria, India, in 1990. He received the B. Tech. degree in electronics and communication engineering from Uttar Pradesh Technical University, Lucknow, in 2010. He is currently pursuing the Ph.D. degree from the Department of Electronics Engineering, Indian Institute of Technology (Indian School of Mines), Dhanbad, India. He joined as a Junior Research Fellow with the Department of Electronics Engineering, Indian Institute of Technology (Indian School of Mines), Dhanbad, in 2014, where he has been a Senior Research Fellow since 2016. He has authored or co-authored over 20 research articles in international/national journals/ conference proceedings. His current research interests involve Metamaterials structures and dielectric resonator antennas.

MOHAMMED MUZAMMIL SANI was born in Jamshedpur, India in 1977. He received the B.Sc. Engineering degree in electronics and communication engineering from Magadh University, Bodh Gaya, India, in 2001, the M.Tech. degree from the National Institute of Technology Rourkela, India, in 2008. Since 2014, he is pursuing the Ph.D. degree with the Department of Electronics Engineering, Indian Institute of Technology (Indian school of mines), Dhanbad. From 2003 to 2009, he was a Lecturer with the Department of Electronics and Communication Engineering, MACET Patna, India. From 2009 to 2011, he was a Lecturer with the Department of College of Computer Science and Information Systems, Jazan University, Jazan, Saudi Arabia. In 2011, he joined as an Assistant Professor with the BA College of Engineering and Technology, Jamshedpur, India. His current research interests in dielectric resonator antennas and its application.

RAGHVENDRA KUMAR CHAUDHARY (S'10–M'13) received the B.Tech. degree from the Institute of Engineering and Technology, Kanpur University, India, in 2007, the M.Tech. degree from the Indian Institute of Technology (BHU), Varanasi, India, in 2009, and the Ph.D. degree from the Indian Institute of Technology Kanpur, India, in 2014. He is currently an Assistant Professor with the Department of Electronics Engineering, Indian Institute of Technology (Indian School of Mines),
Dhanbad, India. He has authored over 122 referred Journal and Conference papers. His current research interests involve metamaterials, dielectric resonators, and computational electromagnetics. He was the recipient of the International Travel Grant form CSIR, DST, and IIT Kanpur, India. He was the recipient of the Best Student Paper Bronze Award at IEEE APACE, Malaysia, in 2010 and also a recipient of the Best Paper Award, ATMS, India, in 2012. He is the potential reviewer of many journals and conferences, such as IEEE TRANSACTIONS on ANTENNAS and PROPAGATION, IEEE ANTENNA and WIRELESS PROPAGATION LETTERS, IET Microwave, Antenna and Propagation, International Journal of RF and Microwave Computer Aided Engineering APS/URSI.